Eur. Phys. J. B (2012) 85: 51
DOI: 10.1140/epjb/e2011-20429-x

THE EUROPEAN PHYSICAL JOURNAL B

Regular Article

Analytic results and weighted Monte Carlo simulations for CDO pricing

M. Stippinger[1], É. Rácz[1,a], B. Vető[2], and Zs. Bihary[3]

[1] Department of Theoretical Physics, Budapest University of Technology and Economics, 8 Budafoki út, 1111 Budapest, Hungary
[2] Department of Stochastics, Budapest University of Technology and Economics, 1 Egry J. u., 1111 Budapest, Hungary
[3] Morgan Stanley Business and Technology Centre, 8 Lechner Ö. fasor, 1095 Budapest, Hungary

Received 5 June 2011 / Received in final form 29 August 2011
Published online 8 February 2012 –

Abstract. We explore the possibilities of importance sampling in the Monte Carlo pricing of a structured credit derivative referred to as *Collateralized Debt Obligation* (CDO). Modeling a CDO contract is challenging, since it depends on a pool of (typically ∼100) assets, Monte Carlo simulations are often the only feasible approach to pricing. Variance reduction techniques are therefore of great importance. This paper presents an exact analytic solution using Laplace-transform and MC importance sampling results for an easily tractable intensity-based model of the CDO, namely the compound Poissonian. Furthermore analytic formulas are derived for the reweighting efficiency. The computational gain is appealing, nevertheless, even in this basic scheme, a phase transition can be found, rendering some parameter regimes out of reach. A model-independent transform approach is also presented for CDO pricing.

1 Introduction

Econophysics literature, especially due to the availability of high-resolution stock exchange trading data, has initially been concerned with interpreting equity stylized facts [1–3] and equity derivatives. The past decade however, has shown a tremendous rise in the trading volume of credit derivatives [4], i.e., products depending on an event like bankruptcy, default or changes in the credit rating of a company or government. The buyer of the protection against such an event transfers his credit risk to the seller, and pays a periodic fee in return, maximally until the maturity of the contract. Although in this setting, credit derivatives are instruments of risk reduction, since it is not necessary to own, e.g., a bond of the companies of interest, they open ground for speculation, too.

The simplest credit derivative is the *Credit Default Swap* (CDS), which is a swap transferring the risk of holding a fixed income product of a single company, such as a bond. In case the company defaults on paying the bond coupons, the buyer of the CDS is entitled to the face value of the bond. The price (the periodic payment to the seller) of a CDS is quoted in bps (basis points), i.e., 10^{-4} of the nominal value of the contract, and is referred to as *CDS spread*. The higher the spread, the riskier the market deems investing in the company in question.

Opposed to CDS-s, structured products depend on the status of many underlying assets (e.g., the bonds of many companies) which, due to the interwoven nature of business relationships and macroeconomic factors, have a complex correlation structure. The subprime mortgage crisis of 2007−2008 has shown that the rising volume of such contracts [4] can lead to unforeseen instabilities.

Monte Carlo simulations are essential in the pricing procedure of structured products since the models used in this context are to complex for analytic assessment. Much effort has been spent on improving different aspects of these MC simulations, like speed and accuracy. An additional important task is calibrating the model parameters to market-observable prices of benchmark instruments. One approach to the latter problem is reweighting MC paths gained using a prior probability measure (weighted Monte Carlo, or WMC, Avellaneda et al. [5] and in the context of credit derivatives Cont and Minca [6]). Our work also involves reweighting MC paths, but the goal is reducing the variance of the Monte Carlo estimates of the expected cashflow, not calibration to market observables. The reweighting scheme is based on the Radon-Nikodým derivative, and is also referred to as importance sampling (see Sect. 4.3 in [7]). Similar investigations have been carried out in the context of different models, for further details, see [8–10].

In this paper, we are dealing with collateralized debt obligations, which are contingent on the default status of the constituents of a reference portfolio, such as Markit iTraxx Europe or CDX NA IG [11]. The contract can basically be viewed as a combination of many CDS-s, however,

[a] e-mail: racze@phy.bme.hu

the net loss on the portfolio is divided into smaller intervals, termed *tranches*. The seller of a CDO tranche pays the excess loss on the portfolio above a threshold (attachment point of the tranche), up to a maximum value (detachment point), and receives in return a periodic payment from the buyer (proportional to the remaining width of the tranche), referred to as CDO tranche *premium*. Standard CDO tranches for the CDX NA IG series include the *equity* (0−3%), the *mezzanine* (3−7%, 7−15%) and the *super senior* (15−100%) tranches. The attachment points of the super senior tranches of other indices range from 15% to 35%; in our work, we used the 30−100% slice as a representative super senior tranche. In the market, these products are quoted in either basis points (10^{-4}, e.g., a spread of 100 basis points means the annual premium payment fraction, although payments are typically made semi-annually), i.e., the value of the periodic payment, or, assuming a fixed premium, the value of the upfront payment (in % of the tranche notional). For the sake of simplicity, we assume zero upfront in each case considered.

Note that the cost functions of buyer/seller are nonlinear, thus, the dependence structure between portfolio elements plays a crucial role in pricing a CDO tranche. "Bottom-up" approaches, including the Gaussian copula model [12] which became infamous during the recent financial crisis [13], try to estimate this dependence structure, and price CDO-s consistently with single name credit defaults swaps. "Top-down" models, in contrast, deal directly with the aggregate loss on the portfolio, thereby decreasing the number of model parameters (in bottom-up approaches, this is done by introducing homogeneity assumptions) and giving up information about component risks (but see the "random thinning" procedure in [14]). In this paper, we consider a simple top-down compound Poisson model in order to retain analytic tractability and demonstrate MC possibilities.

The paper is organized as follows: Section 2 summarizes model details and the relevant quantities. Section 3 introduces a general method for CDO pricing for models including a constant interest rate and deduces analytic formulas for the cash flow of the CDO contract in the Poissonian case. Section 4 turns to presenting the possibilities of the Monte Carlo simulation and importance sampling, which, for this simple model, can again be analytically verified.

2 Basic concepts

2.1 Collateralized debt obligation – the basic model

Let us assume that the CDO is based on a homogeneous pool of companies, which, for the sake of simplicity, is homogeneous, i.e., the number of default events is proportional to the loss on portfolio value. Furthermore, we assume that the losses on the portfolio are continuous. This is a natural simplification for typical index portfolios of ∼100 entities.

This model is based on a single default process D_t which is a compound Poisson process in the following sense: the default events occur according to a simple Poisson process of intensity ρ, and during the ith event, a fraction J_i of the companies default. The jump sizes J_i are independent and identically distributed random variables of exponential distribution with parameter λ, i.e., $\mathbf{P}(J_i < x) = 1 - e^{-\lambda x}$. We also use the notation $\mu = \lambda^{-1}$ for the expected value of the jumps. We assume that $\{J_i\}_i$ are also independent from the jump times.

We considered two natural ways to define the actual loss process with values in $[0, 1]$. The first one is referred to as the linear specification given by

$$L_t^{\mathrm{lin}} := \min(D_t, 1).$$

The exponential specification

$$L_t^{\exp} := 1 - \exp\{-D_t\} \tag{1}$$

is obtained by a smooth transformation from D_t. For small values of D_t, the two quantities $L_t^{\exp}$ and D_t are close, which is the typical case for the relevant parameter regimes. In what follows, we use the exponential specification and omit the superscript ($L_t^{\exp} \to L_t$), and we say that, at time t, an L_t proportion of the companies defaulted.

The buyer of the a CDO tranche $[a, d]$ makes periodic payments (called *premium leg*) proportional to the *outstanding notional* (the remaining width) of the tranche until either the maturity M (the expiry of the contract) is reached or the loss exceeds the detachment point. In the analytic calculations that follow in Section 3, we will assume a premium payment that is continuous in time. This assumption is of course not realistic, however, as comparisons with computer simulation results (Sect. 4) show, it does not have a serious effect on the present values of the premium and default legs. The seller of the protection pays the *default leg* after each default event, which is the increment of $\min\{L_t, d\} - \min\{L_t, a\}$.

The default of a company does not mean that it becomes entirely worthless, a fraction $\tilde{r}$ of its original value is recovered, i.e., the portfolio loss L_t increases by a $1 - \tilde{r}$ proportion of the jump which occurred at time t. In the simplest setting, the recovery $\tilde{r}$ is a deterministic constant $\tilde{r} \in [0, 1)$ (see [12,15,16] for example). In this paper, we simply assume that $\tilde{r} = 0$.

2.2 Relevant quantities

Let the interest rate r be constant in time. For a tranche $[a, d]$, we denote by

$$\ell_t^{a,d} = \min(L_t, d) - \min(L_t, a) \tag{2}$$

the loss on this tranche at time t. The phrase tranche loss is often used in the literature for $\ell_M^{a,d}$ the total loss at the maturity.

The default leg present value (`defPV`) of a tranche is approximately the expected present value of the tranche

loss, more precisely, the increments of the loss are discounted. In mathematical terms,

$$\texttt{defPV} = \mathbf{E}\left(\int_0^M e^{-rt}\, d\ell_t^{a,d}\right) \tag{3}$$

which is meant as a Stieltjes integral. The dependence of the defPV on the tranche is suppressed in the notation.

The premium leg present value (premPV) is the expected present value of the total amount of the periodic payment by the protection buyer. The annual payment is $\texttt{spread} \times ON_t$ where the spread is given in basis points (bps) and fixed in the contract. ON_t is the outstanding notional of the tranche $[a, d]$ at time t, i.e.

$$ON_t = d - a - \ell_t^{a,d}.$$

Hence,

$$\texttt{premPV} = \texttt{spread} \times \mathbf{E}\left(\int_0^M e^{-rt} ON_t\, dt\right) \tag{4}$$

where the expectation on the right-hand side is denoted by premPV1bp.

The aim of CDO pricing is to give a good estimate of the fair value of the spread (and upfront) for given tranches. Therefore, the equation

$$\texttt{defPV} = \texttt{spread} \times \texttt{premPV1bp}\ (+\texttt{upfront})$$

has to be satisfied, since the left-hand side is the expected income of the protection buyer, whereas the right-hand side is that of the protection seller. The problem is now reduced to finding the values defPV and premPV1bp.

Throughout the paper, we will also use the notation

$$X^{(\texttt{def})} := \int_0^M e^{-rt}\, d\ell_t^{a,d}, \tag{5}$$

$$X^{(\texttt{prem})} := \int_0^M e^{-rt} ON_t\, dt, \tag{6}$$

which stand for the present value of the tranche loss and that of the total amount of premium leg paid by the protection buyer respectively. Note that these are random variables, and their expectations are

$$\mathbf{E}\left(X^{(\texttt{def})}\right) = \texttt{defPV}, \tag{7}$$

$$\mathbf{E}\left(X^{(\texttt{prem})}\right) = \texttt{premPV1bp}, \tag{8}$$

compare with (3) and (4).

We define

$$\mathfrak{a} := -\ln(1-a), \tag{9}$$

$$\mathfrak{d} := -\ln(1-d). \tag{10}$$

Due to (1), the event $\{L_t > a\}$ is equal to $\{D_t > \mathfrak{a}\}$. The same hold with d and $\mathfrak{d}$ respectively. This notation serves to reduce the length of subsequent formulas.

3 Analytic approach

In the compound Poissonian case, we can derive explicit formulas for the relevant quantities defPV and premPV1bp. The expressions contain an infinite series representation, which converges faster than exponential, therefore, our method provides a promising approach to CDO pricing. The basic idea of the computations is that we decompose the underlying expectation according to the first passage of certain levels of loss.

3.1 The defPV and premPV1bp expressed with the first passage time

The loss L_t is an exponential transformation of the compound Poisson process D_t, see (1), and the computations can be done in terms of D_t. Hence, we introduce

$$T_h := \min\{t \geq 0 : D_t \geq h\}$$

the first passage time of level h for D_t. It turns out that the quantities defPV and premPV1bp can be expressed by the integral of the function

$$\varphi_r(h, M) := \mathbf{E}\left(e^{-rT_h} \mathbb{1}(T_h < M)\right) \tag{11}$$

which is a modified Laplace transform of the first passage time, and $\mathbb{1}(\cdot)$ denotes the indicator function. Therefore, knowing the function φ_r is enough to determine defPV and premPV1bp and also the fair value of spread and upfront.

It is not difficult to show that instead of the original definition of defPV in (3) where the increments of loss are added, with a new approach, an integration along the vertical axis can be done, see also Figure 1. We obtain

$$\begin{aligned}\texttt{defPV} &= \mathbf{E}\left(\int_a^d e^{-r\min\{t\geq 0: L_t \geq x\}} \mathbb{1}(x < L_M)\, dx\right)\\ &= \mathbf{E}\left(\int_{\mathfrak{a}}^{\mathfrak{d}} e^{-rT_h} \mathbb{1}(T_h < M)\, e^{-h}\, dh\right)\\ &= \int_{\mathfrak{a}}^{\mathfrak{d}} \varphi_r(h, M)\, e^{-h}\, dh\end{aligned} \tag{12}$$

after a change of variable under the integral sign ($x \to h = -\ln(1-x)$), which corresponds to considering the compound Poisson process D_t itself instead of L_t.

Similarly, definition (4) of the premPV1bp is replaced by

$$\begin{aligned}\texttt{premPV1bp} &= \mathbf{E}\left(\int_a^d \int_0^{\min\{0\leq t\leq M: L_t \geq x\}} e^{-rs}\, ds\, dx\right)\\ &= \mathbf{E}\left(\int_{\mathfrak{a}}^{\mathfrak{d}} \int_0^{\min(T_h, M)} e^{-rs}\, ds\, e^{-h}\, dh\right)\\ &= \mathbf{E}\left(\int_{\mathfrak{a}}^{\mathfrak{d}} \frac{1 - e^{-r\min(T_h, M)}}{r} e^{-h}\, dh\right).\end{aligned} \tag{13}$$

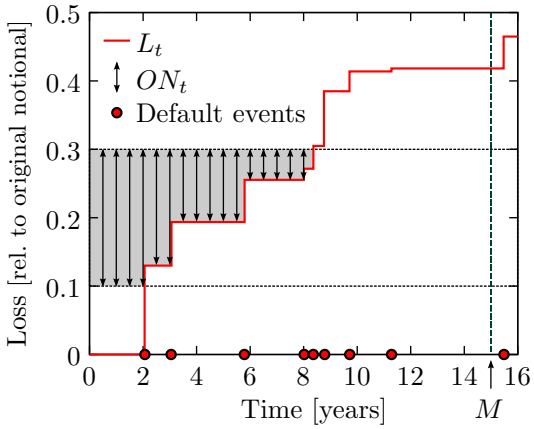

Fig. 1. (Color online) A sample scenario of the loss process L_t. The jumps in the solid red line indicate the default events occurring according to a Poisson process of intensity ρ. Assuming continuous payment, the default leg present value `defPV` is the sum of the discounted increments of the loss process L_t (see Eq. (12)) and the the premium leg present value `premPV1bp` is related to the grey area (in case $r = 0$, they coincide, see Eq. (13)).

In terms of Figure 1, formulas (4) and (13) give the indicated area in two different ways. After straightforward manipulations, one obtains from (13) that

$$\begin{aligned}\texttt{premPV1bp} = {} & \frac{1}{r}\left(1 - e^{-rM}\right)(d-a) \\ & + \frac{e^{-rM}}{r}\int_{\mathfrak{a}}^{\mathfrak{d}} \varphi_0(h,M)\, e^{-h}\, dh \\ & - \frac{1}{r}\int_{\mathfrak{a}}^{\mathfrak{d}} \varphi_r(h,M)\, e^{-h}\, dh, \end{aligned} \tag{14}$$

with the unknown function φ_r depending on the details of the model. An important remark is that formulas (12) and (14) are valid for *any* distribution of the process D_t, not only for the compound Poissonian case, we assumed only a constant interest rate and continuous payment possibilities for both sides (it is simple to generalize the results for deterministic interest rate functions $e^{-rt} \to \exp\{-\int_0^t r(s)\, ds\}$, but we omit this possibility in the present paper). Using the present approach, for any distribution of D_t, it is enough to determine the function φ_r for pricing a CDO. In the next subsection, we calculate φ_r in the compound Poissonian case.

3.2 Partial differential equation for the Laplace transform of the first passage time

For the compound Poisson process D_t, a series representation of φ_r can be given as follows. In order to avoid later confusions, we fix the value of the interest rate r, and we suppress the subindex of φ. The expectation in (11) can be decomposed according to the time and the size of the first jump of the process D_t since these are independent exponential random variables with parameter ρ and λ respectively. After change of variable, one can obtain the integral equation

$$\begin{aligned}\varphi(h,M) = {} & \rho e^{-(\rho+r)M} e^{-\lambda h} \\ & \times \int_0^M e^{(\rho+r)y}\left(\lambda\int_0^h e^{\lambda x}\varphi(x,y)\, dx + 1\right) dy \end{aligned} \tag{15}$$

using the memoryless property of the exponentials. Differentiating (15), we can deduce the partial differential equation

$$\partial^2_{hM}\varphi + \lambda\partial_M\varphi + (\rho+r)\partial_h\varphi + \lambda r\varphi = 0. \tag{16}$$

One boundary value is obviously

$$\varphi(h,0) = 0. \tag{17}$$

One has to be more careful at the other one. By definition, the function is constant 1 along the line $h = 0$, but the bivariate function $\varphi(h,M)$ is not continuous here. Therefore, we redefine φ at the boundary, or, more precisely, we can say that the definition (11) is valid only if $h > 0$, and we extend the function continuously. Since as $h \downarrow 0$, the probability that the first jump exceeds h tends to 1, the boundary value is

$$\begin{aligned}\varphi(0,M) = \lim_{h\downarrow 0}\varphi(h,M) &= \int_0^M e^{-ry}\rho e^{-\rho y} dy \\ &= \frac{\rho}{\rho+r}\left(1 - e^{-(\rho+r)M}\right). \end{aligned} \tag{18}$$

3.3 Solution of the PDE

Equation (16) is a second order hyperbolic partial differential equation, which contains extra terms of lower order. One way of solving it is performing Laplace transformation in both variables. Let

$$\varphi_{st} := \int_0^\infty\int_0^\infty e^{-sh}e^{-tM}\varphi(h,M)\, dh\, dM$$

be the Laplace transform. We will also use the functions

$$\begin{aligned}\varphi_s(M) &:= \int_0^\infty e^{-sh}\varphi(h,M)\, dh, \\ \varphi_t(h) &:= \int_0^\infty e^{-tM}\varphi(h,M)\, dM \end{aligned}$$

for computing the Laplace transforms of $\partial^2_{hM}\varphi$, $\partial_h\varphi$ and $\partial_M\varphi$. They can be given by integration by parts. In the calculation, the Laplace transforms of the boundary values (17) and (18) also appear.

The Laplace transform of equation (16) is written as

$$\begin{aligned} & st\varphi_{st} - t\frac{\rho}{t(t+\rho+r)} + \lambda t\varphi_{st} \\ & \quad + (\rho+r)\left(s\varphi_{st} - \frac{\rho}{t(t+\rho+r)}\right) + \lambda r\varphi_{st} = 0. \end{aligned}$$

The unknown function φ_{st} can be expressed easily:

$$\varphi_{st} = \frac{\rho}{t}\,\frac{1}{st+\lambda t+(\rho+r)s+\lambda r}. \tag{19}$$

The elimination of variable t can be done by using the identity

$$\int_0^\infty e^{-px}\frac{1-e^{-\alpha x}}{\alpha}\,dx = \frac{1}{p(p+\alpha)}$$

with $\alpha = ((\rho+r)s+\lambda r)/(s+\lambda)$. We get

$$\varphi_s(M) = \frac{\rho}{\rho+r}\frac{1}{s+\frac{\lambda r}{\rho+r}} \times\left(1-\exp\left(-(\rho+r)M+\frac{\lambda\rho M}{s+\lambda}\right)\right). \tag{20}$$

The second inversion is not completely obvious. The difficulty is that, in the second term in (20), the variable s appears in two different places: in the denominator of the prefactor $1/(s+\lambda r/(\rho+r))$ and in the exponential as well.

We could use the general identity

$$\int_0^\infty e^{-px}\left(e^{\beta x}\int_0^x f(y)\,dy\right)dx = \frac{\int_0^\infty e^{-(p-\beta)x}f(x)\,dx}{p-\beta} \tag{21}$$

with $\beta = -\lambda r/(\rho+r)$ to proceed. Then the problem reduces to finding the inverse Laplace transform of the function

$$g_s(M) = \exp\left(\frac{\lambda\rho M}{s+\frac{\lambda\rho}{\rho+r}}\right)$$

in the s variable where s occurs only once. It can be solved by considering the series expansion of the exponential and by performing the inversion for each term individually using the general formula

$$\int_0^\infty e^{-px}\left(\frac{x^{n-1}}{(n-1)!}e^{-\alpha x}\right)dx = \frac{1}{(p+\alpha)^n}.$$

One may notice that for each term of the sum in the series expansion, we get functions of the form $x\mapsto cx^{n-1}e^{-\nu x}$. These are to be integrated by the left-hand side of (21) in place of f. Hence, we also use the following series representation of the lower incomplete gamma function:

$$\int_0^x t^{n-1}e^{-\nu t}\,dt = \frac{(n-1)!}{\nu^n}\left(1-e^{-\nu x}\sum_{k=0}^{n-1}\frac{(\nu x)^k}{k!}\right).$$

The resulting formula is

$$\varphi_r(h,M) = \frac{\rho}{\rho+r}e^{-\lambda h-(\rho+r)M} \times\sum_{n=1}^{\infty}\frac{(\rho+r)^nM^n}{n!}\sum_{k=0}^{n-1}\left(\frac{\lambda\rho h}{\rho+r}\right)^k\frac{1}{k!}. \tag{22}$$

It is not hard to see that the solution (22) indeed satisfies equation (16) along with the boundary values (18) and (17). One more important special case is if $r=0$. The (22) reduces to

$$\varphi_0(h,M) = \sum_{n=1}^{\infty}e^{-\rho M}\frac{(\rho M)^n}{n!}\sum_{k=0}^{n-1}e^{-\lambda h}\frac{(\lambda h)^k}{k!} \tag{23}$$

which can be verified intuitively as follows. The left-hand side of (23) is equal to $\mathbf{P}(T_h < M)$ by definition. The right-hand side is the sum of the weights of those trajectories of D_t which give rise to the event $\{T_h < M\}$. Assume that D_t has n jumps in the interval $[0,M]$. The jump sizes can be generated by a Poisson point process with intensity λ along the vertical axis. $T_h < M$ is satisfied if and only if this Poisson process has k point in $[0,h]$ with $0\le k<n$. In the general $r>0$ case, the same factors as on the right-hand side of (23) appear in the formula, but there is no explicit probabilistic interpretation of (22).

The benefit of the computations is that, with (22), the value of `defPV` and `premPV` are known explicitly using (12) and (14). The expression (22) is computationally stable because of the factorial in the denominator. This new method gives an unbiased answer also for those tranches for which one cannot guarantee enough sample paths with the usual Monte Carlo simulation. In these parameter regimes (e.g., pricing a super senior tranche), the results can be compared to those of the weighted Monte Carlo simulation.

4 Monte Carlo simulation

This section presents a Monte Carlo study of the compound Poissonian case (Sect. 2.1) that might provide a better understanding of importance sampling for more complex models as well. Although admittedly unrealistic, the model used captures the two basic quantities accessible in any top-down model, namely event frequency and size. Its simplicity allowed not only an analytic solution but, as we shall see in Section 4.2, an analytic treatment of the importance sampling procedure as well.

From the technical point of view, there are two basic approaches to the MC treatment of CDO models:

- the "path-based" approach calculates each quantity of interest for all generated paths, and afterwards calculates the statistics of the gained data sets;
- the "surface-based" approach estimates the time-dependent probability density function of the portfolio loss, i.e., a simple matrix, as in Figure 2.

Although both methods provide the present values of the premium and default legs, for our purposes, the former is more suitable since our aim is to reduce the number of Monte Carlo paths necessary to obtain the price of senior tranches with a certain precision.

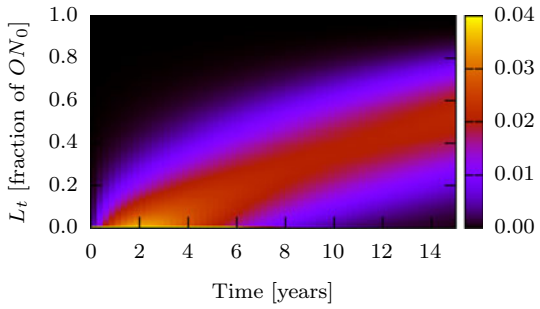

Fig. 2. (Color online) Loss surface of the compound Poisson process with intensity $\rho = 0.5$ and exponential jump sizes of parameter $\lambda = 10$ (expected value $\frac{1}{\lambda} = 0.1$) generated by 10^6 Monte Carlo paths. The $L_t = 0$ stripe is not shown, because it contains much larger probabilities than the central region, and would therefore obstruct visibility.

Monte Carlo with paths

For the ith realization of the process, the cash flow values are calculated as follows:

$$X_i^{(\mathtt{def})} = \sum_{k=1}^{k_{\max}} e^{-rt_k} \left(\ell_{t_k}^{a,d} - \ell_{t_{k-1}}^{a,d} \right) \tag{24}$$

$$X_i^{(\mathtt{prem})} = \sum_{k=1}^{k_{\max}} e^{-rt_k} \, ON_{t_k}, \tag{25}$$

with $0 = t_0, t_1, \ldots, t_{k_{\max}} = M$ representing an equally spaced time grid. The necessity of discretization is commonly a drawback of simulations, in our case, however, it is realistic since CDO payments are typically transferred quarterly. For efficiency reasons, the generated paths should be evaluated simultaneously for all tranches $[a, d]$ of interest. The individual financial values $X_i^{(\mathtt{def})}$ and $X_i^{(\mathtt{prem})}$ per tranche are subject to a statistical analysis.

4.1 Reweighted Monte Carlo

The aim of reweighting is to reduce the computational time needed for finding the expected present values of the premium and the default. Applying reweighting, the program generates Monte Carlo paths with an altered parameter set of the compound Poisson model, that is, with an altered intensity ρ' and an altered expected jump size $\frac{1}{\lambda'}$. Using parameters which describe a relatively calm economic situation, senior tranches are typically not reached by MC paths, i.e., one obtains a poor estimate of their price. The idea is to simulate paths using a parameter set describing a more severe situation, and reweight them to preserve the original expected value while reducing the variance.

The reweighting relies on the Radon-Nikodým derivative, the derivative of one probability measure with respect to another [7]. To get the appropriate weights, we have to calculate it for the real with respect to the altered one.

We write the probability of realization of a path considering that the N_M jumps occur in small intervals $(t_j, t_j + dt)$ $j = 1, \ldots, N_M$ with the given intensity ρ and that there is no jump outside of these intervals. We handle the jump sizes in a similar way under the condition that the number of jumps is already given by the Poisson process (we introduce the notations $t_0 = 0$ and $D_0 = 0$):

$$\begin{aligned} \mathbf{P}(\text{path}) = &\prod_{i=1}^{N_M} \left(e^{-\rho(t_i - t_{i-1})} \rho \, dt \right) e^{-\rho(M - t_{N_M})} \\ &\times \prod_{i=1}^{N_M} \left(e^{-\lambda(D_{t_i} - D_{t_{i-1}})} \lambda \, dh \right), \end{aligned} \tag{26}$$

with the first term corresponding to the pdf of the intervals between jumps, the second to the probability that there is no event between the last jump and the maturity M and the third to the pdf of the jump sizes. It is straightforward to generalize the latter equation for arbitrary renewal processes, one only has to change the terms to the jump time and size distributions of interest.

The Radon-Nikodým derivative of one probability measure with respect to another one is the ratio of the weights of the same path given in (26) under the two measures, and for a path with N_M jumps is given by

$$\begin{aligned} R(N_M, D_M) &= \frac{d\mathbf{P}}{d\mathbf{P}'}(N_M, D_M) \\ &= \left(\frac{\rho\lambda}{\rho'\lambda'} \right)^{N_M} e^{-(\rho - \rho')M - (\lambda - \lambda')D_M} \end{aligned} \tag{27}$$

where $\mathbf{P}$ and $\mathbf{P}'$ are respectively the measures parametrized by the real and the alternative parameters. This quantity is both calculable analytically as a random variable and numerically for a specific Monte Carlo path. The Monte Carlo simulation calculates $R(\text{path})$ step by step, during the generation of a path. Starting from the value 1, at each jump in the path, the program multiplies the stored value by the contribution of that jump (terms under the product signs in (26)); at the end of the path, it multiplies the value by the contribution which describes that no more events happened until the maturity (middle factor on the right-hand side of (26)).

In mathematical terms, the random variable simulated under the altered measure $\mathbf{P}'$ is RX (with X standing for either premium or default leg), thus, its observable variance is

$$\begin{aligned} \mathbf{Var}'(RX) &= \mathbf{E}'(R^2X^2) - (\mathbf{E}'RX)^2 \\ &= \mathbf{E}(RX^2) - (\mathbf{E}X)^2, \end{aligned} \tag{28}$$

since $\mathbf{E}'(RX) = \mathbf{E}(X)$, by definition of the Radon-Nikodým derivative.

Being able to measure the variance, we use this feature to find the optimal parameter set for the speed of convergence and then we perform importance sampling with those parameters.

4.2 Reweighting: analytic approach

In this section, we analytically evaluate the variance of the reweighted default considering the compound Poisson

process D_t where the jump times follow a Poisson process with intensity ρ and the sizes of the jumps are independent exponentially distributed random variables with parameter λ, which are independent of the Poisson point process as well. Then we calculate the expected loss and its variance analytically with the assumption that there are no discount factors, i.e., $r = 0$.

Recall (5), and note that in case $r = 0$, we have

$$\begin{aligned} X^{(\mathtt{def})} &= (L_M - a) \cdot \mathbb{1}\left(L_M \in [a, d]\right) \\ &\quad + (d - a) \cdot \mathbb{1}\left(L_M > d\right) \\ &= \left(1 - e^{-D_M} - a\right) \cdot \mathbb{1}\left(D_M \in [\mathfrak{a}, \mathfrak{d}]\right) \\ &\quad + (d - a) \cdot \mathbb{1}\left(D_M > \mathfrak{d}\right). \end{aligned} \tag{29}$$

Then

$$\mathtt{defPV} = \mathbf{E}\left(X^{(\mathtt{def})}\right) = \mathbf{E}'\left(RX^{(\mathtt{def})}\right), \tag{30}$$

where the second equality holds by the definition of the measure change. The important quantity here is the error of the Monte Carlo simulation carried out with importance sampling, thus, our aim is to calculate the variance given in (28).

The joint density of N_M (number of jumps) and D_M is given by

$$\begin{aligned} f_*(n,h) &= \mathbf{P}_*(N_M = n, D_M \in (h, h + dh)) \\ &= e^{-\rho_* M} \frac{(\rho_* M)^n}{n!} h^{n-1} e^{-\lambda_* h} \frac{(\lambda_*)^n}{(n-1)!}\, dh + o(dh) \\ &= e^{-\lambda_* h - \rho_* M} \frac{(\rho_* M \lambda_*)^n h^{n-1}}{n!(n-1)!}\, dh + o(dh) \end{aligned}$$

where $*$ can stand for either altered or real. This bivariate joint probability density function is composed of the product of the probability density functions of a POI$(\rho_* M)$ describing n events until the maturity and a $\Gamma(\lambda_*, n)$ describing the conditional probability of arriving in $(h, h + dh)$ having n jumps. Please note that this is a defective probability distribution, the missing mass is $\mathbf{P}_*(D_M = 0) = e^{-\rho_* M}$.

Using (29), one can calculate

$$\begin{aligned} \mathbf{E}\left(X^{(\mathtt{def})}\right) &= (1 - a) \int_{\mathfrak{a}}^{\mathfrak{d}} \sum_{n=1}^{\infty} f(n,h)\, dh \\ &\quad - \int_{\mathfrak{a}}^{\mathfrak{d}} e^{-h} \sum_{n=1}^{\infty} f(n,h)\, dh \\ &\quad + (d - a) \int_{\mathfrak{d}}^{\infty} \sum_{n=1}^{\infty} f(n,h)\, dh, \end{aligned} \tag{31}$$

similarly, for the variance,

$$\begin{aligned} \mathbf{E}\left(R\left(X^{(\mathtt{def})}\right)^2\right) &= \int_{\mathfrak{a}}^{\mathfrak{d}} \sum_{n=1}^{\infty} e^{-2h} R(n,h) f(n,h)\, dh \\ &\quad - 2(1 - a) \int_{\mathfrak{a}}^{\mathfrak{d}} \sum_{n=1}^{\infty} e^{-h} R(n,h) f(n,h)\, dh \\ &\quad + (1 - a)^2 \int_{\mathfrak{a}}^{\mathfrak{d}} \sum_{n=1}^{\infty} R(n,h) f(n,h)\, dh \\ &\quad + (d - a)^2 \int_{\mathfrak{d}}^{\infty} \sum_{n=1}^{\infty} R(n,h) f(n,h)\, dh \end{aligned} \tag{32}$$

where the integrals can be expressed in terms of incomplete gamma functions, since the dependence of the integrands on h is a product of a polynomial and an exponential function, that is, they are of the form

$$\int_l^u e^{-\nu h} h^{n-1}\, dh.$$

Deriving the result is not extremely difficult but rather technical, therefore we omit these details.

We remark one more interesting feature of the expectation in (32) which is the appearance of *phase transition*. In the first two terms on the right-hand side of (32), the integrals are not necessarily finite (for the other term, we do not have this issue). It can be verified by analyzing the exponential factors in h of the integrand. In the first term on the right-hand side of (32), $R(n,h)$ contributes with $e^{-(\lambda - \lambda')h}$, whereas $f(n,h)$ gives an exponential factor of $e^{-\lambda h}$. The product of these two is clearly $e^{-(2\lambda - \lambda')h}$. Hence, the first integral in (32) is finite if and only if

$$2\lambda - \lambda' > 0 \quad \Longleftrightarrow \quad \mu' > \frac{1}{2}\,\mu.$$

The consequence of this phase transition is that if one intends to apply the importance sampling method for a more complex model, where such divergences cannot be assessed analytically, one has to take care to identify the permissible parameter regime that can actually be worked with.

4.3 Monte Carlo results

In this section, we discuss the simulation results and compare them to the analytic solution. For illustration purposes, we have chosen from the standard tranches (see Sect. 1) the *super senior tranche* ($a = 0.3$, $d = 1$). For each Monte Carlo simulation we used $n = 10^6$ paths and no recovery ($\tilde{r} = 0$).

Approximating the model parameters in a calm economic situation by:

$$\rho = 0.05\ \frac{\text{events}}{\text{year}} \tag{33}$$

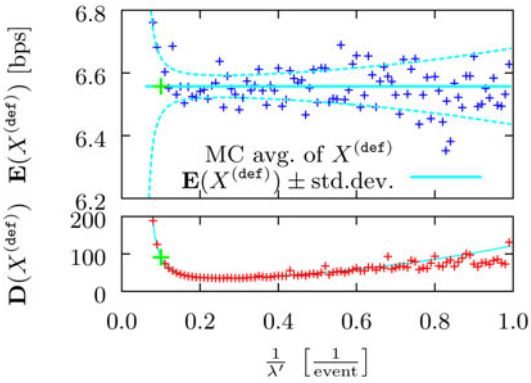

Fig. 3. (Color online) The measured average and standard deviation of $X^{(\mathtt{def})}$ for the super senior tranche as a function of $\frac{1}{\lambda'}$, with $\rho' = \rho$, ($\lambda = 10$, $\rho = 0.05$). The average (**E** axis) and standard deviation (**D** axis) of the $X^{(\mathtt{def})}$ are given in basis points. The variance remarkably decreases for $\frac{1}{\lambda'} \approx 2.8 \times \frac{1}{\lambda} = 0.28$.

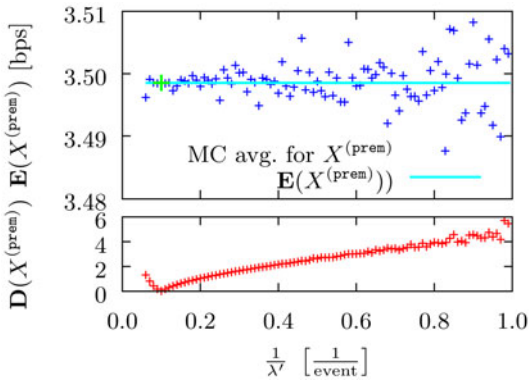

Fig. 4. (Color online) The measured average and standard deviation of $X^{(\mathtt{prem})}$ for the super senior tranche as a function of $\frac{1}{\lambda'}$, with $\rho' = \rho$, ($\lambda = 10$, $\rho = 0.05$). The average (**E** axis) and standard deviation (**D** axis) of $X^{(\mathtt{prem})}$ are given for a 1 basis point spread. The estimation of the premium leg present value was not improved for the super senior tranche. We have no analytic formula for `premPV1bp`.

for the intensity of the compound Poisson process and about

$$\frac{1}{\lambda} = 0.10 \, \frac{\text{fraction of the original notional}}{\text{event}} \tag{34}$$

for the expected number of defaults (i.e., 10 assets are expected to default per event for a 100-element portfolio). The standard maturity is

$$M = 5 \text{ years}. \tag{35}$$

The benefit of the reweighting procedure is given quantitatively by the well-known fact that the standard deviation of a sample average (of independent realizations of a random variable) is $\frac{\sigma}{\sqrt{n}}$, where σ is the standard deviation of the random variable and n is the number of realizations used to estimate its mean. Thus, the number of MC paths necessary to achieve a fixed precision is proportional to the variance. We define the gain in the number of paths consequently as

$$G_{\text{num}} := \frac{n}{n'} = \frac{\sigma^2}{\sigma'^2}. \tag{36}$$

The parameter set (ρ, λ) corresponds to relatively rare events (one event per four realizations on average) and small chance to touch the super senior tranche. Thus it is qualitatively clear that to obtain a lower variance of its present value, the alternative parameters have to fall in $\{(\rho', \lambda') : \rho' > \rho, \lambda' < \lambda\}$.

We executed a simulation for the given ρ, $\frac{1}{\lambda}$ and $M = 5$ to study the effect of the *jump size parameter* on the standard deviation. The results for the super senior tranche are presented in Figures 3 and 4. In both diagrams, the top part represents the MC average and the analytic expected value, as well as the analytically calculated Monte Carlo error marking the confidence interval. This error is given by the standard deviation of the $X^{(\mathtt{def})}$ for one path divided by $\sqrt{n} = 1000$. The bottom part of the diagrams retraces the analytic and the empirical value of the same standard deviation to facilitate the comparison. We performed the same comparison for each standard tranche as well as the index tranche, and observed a very good match of analytic and simulation results. Moreover, standard deviations of the default leg present value could be decreased in each case except for the equity tranche. The maximal gain for the super senior tranche is obtained for $\frac{1}{\lambda'} = 0.28$ where the variance was reduced to 14% of its original value. In contrast, `premPV1bp` cannot be estimated more accurately than in the non-reweighted case, however, $X^{(\mathtt{prem})}$ can already be easily and accurately estimated without reweighting, as shown in Figure 3. Even the relative error ($\frac{\text{std. dev.}}{\text{expected v.}}$) of `premPV1bp` increased by the reweighting procedure remains an order below the relative error of `defPV`. Thus, the importance sampling scheme improves the more relevant source of uncertainty in the pricing procedure.

The same investigation was carried out along the ρ' axis; the results for the super senior tranche are shown in Figures 5 and 6. We observe an equally good match of the analytic and numerical (path) approach as previously. In this case, all tranches exhibit a gain in precision with growing process intensity (which is no wonder, since a larger intensity corresponds to more events until maturity is reached, and consequently a lower variance of the averages). The maximal gain for the super senior tranche is obtained for $\rho' = 0.23(5)$ where the variance was reduced to 30% of its original value.

Although by increasing ρ we can gain on the number of Monte Carlo paths, the gain on computation power is not so evident. On average, each path contains $M\rho'$ jumps which need to be generated and kept account of. An explicit chronometry was done where the process' real computational time on the CPU was collected (not the clock ticks during the execution because the computer could do other things in the background). The execution time for increased ρ'-s is plotted in Figure 7 and is linear in ρ'.

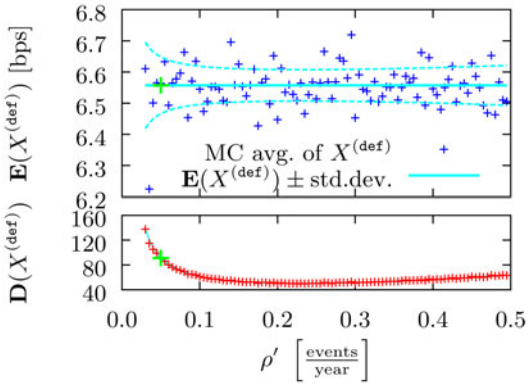

Fig. 5. (Color online) The measured average and standard deviation of $X^{(\mathtt{def})}$ for the super senior tranche as a function of ρ', with $\lambda' = \lambda$, ($\lambda = 10$, $\rho = 0.05$). The average (**E** axis) and standard deviation (**D** axis) of the $X^{(\mathtt{def})}$ are given in basis points. The variance decreases most if $\rho' \in (4\rho, 5\rho) = (0.20, 0.25)$.

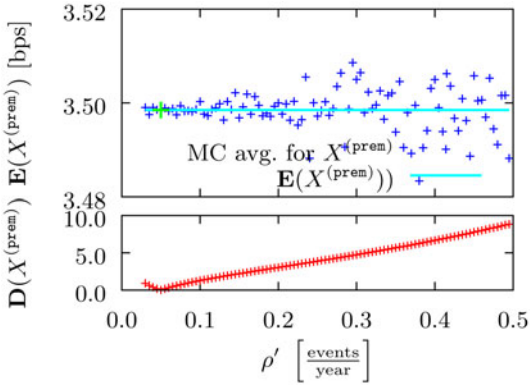

Fig. 6. (Color online) The measured average and standard deviation of $X^{(\mathtt{prem})}$ for the super senior tranche as a function of ρ', with $\lambda' = \lambda$, ($\lambda = 10$, $\rho = 0.05$). The average (**E** axis) and standard deviation (**D** axis) of $X^{(\mathtt{prem})}$ are given for a 1 basis point spread. The estimation of the premium leg present value was not improved for the super senior tranche.

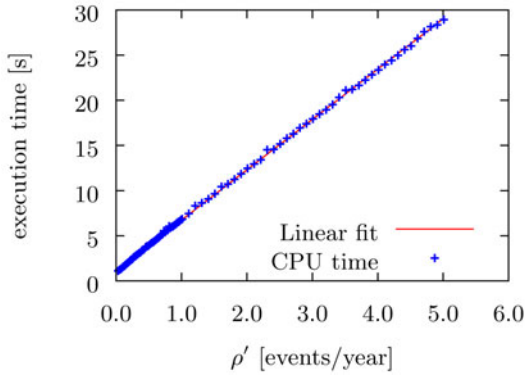

Fig. 7. (Color online) The computational time as a function of the reweighting parameter ρ', which denotes the Poisson process intensity. The points fit on a line of equation $t = c + b\rho'$ where $c = 1.1(67)$ is the average initialization cost of the 10^6 MC paths and $b = 5.57(1)$ is the time consumed by processing the jumps.

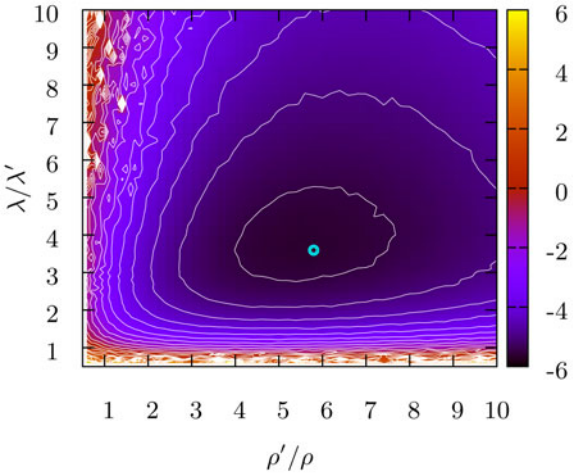

Fig. 8. (Color online) The magnitude of the gain $-\log_2 G_{\mathrm{num}}$ for the super senior tranche in the `defPV` measurement, given in number of Monte Carlo paths as a function of the reweighting parameters: ρ' denotes the altered Poisson process intensity, $\frac{1}{\lambda'}$ the altered expected jump size. The real process uses the real world parameters described in (33) to (35). The variance decreases for the super senior tranche by increasing the intensity and the jump size to 2−6 times of their original value.

With regard to this fact the gain in computational time can be defined as

$$G_{\mathrm{time}} = \frac{t_{\mathrm{comp}}}{t'_{\mathrm{comp}}} = \frac{\sigma^2}{\sigma'^2}\frac{\rho'}{\rho}, \tag{37}$$

where $'$ stands for the reweighted simulation's results, σ denotes the standard deviation of the measured quantity ($X^{(\mathtt{def})}$ or $X^{(\mathtt{prem})}$) and ρ denotes the Poisson process intensity. This effect is not present in the case of $\frac{1}{\lambda'}$ because higher jumps do not provoke more events – they only result in larger numeric values.

To find the optimum with respect to the quantities defined in (36) and (37), we analyzed the $G_{\mathrm{num}}(\rho', 1/\lambda')$ and $G_{\mathrm{time}}(\rho', 1/\lambda')$ maps (Figs. 8 and 9). We can conclude that, in both specifications, the Monte Carlo reweighting scheme can be successfully applied. For the pricing of the super senior tranche the total gain in computer time reaches $G_{\mathrm{time}} = 12.4$, which is more than appealing. The gain in the number of paths was at least $G_{\mathrm{num}} = 3.0$, this minimum appeared at the equity tranche. The numerical results are summarized in Table 1. According to analytic considerations, the functions are smooth, this seems to be satisfied in our Monte Carlo simulation figures, except for the region of rare but large jumps. This is explained by the relatively small number of paths (10^5) being simulated, an order less than for Figures 3 to 6. This number is, however, justified, because the full map with this acceptable resolution ($\sim 10^4$ points) is calculated in more than an hour on a state-of-the-art computer, the optimal sampling of this map is out of the scope of the current paper.

We would like to assure the reader that, in accordance with the analytic results that found a divergence for the $\lambda/\lambda' < 1/2$ regime, the $\lambda/\lambda' \in [0, 0.5]$ margins on the

Table 1. The optimum of the gains G_{time} and G_{num} for `defPV` measurement. The reweighting parameters: ρ' denotes the Poisson process intensity, $\frac{1}{\lambda'}$ the expected jump size. The lowest gain appears for the equity tranche ($a = 0$, $d = 0.03$), the highest for the super senior tranche ($a = 0.3$, $d = 1$). The real process uses the real world parameters described in (33) to (35) as $\rho = 0.05\frac{\text{event}}{\text{year}}$, $\frac{1}{\lambda} = 0.1\frac{\text{original notional}}{\text{event}}$, $M = 5$ years. The index tranche shows a comportment between the equity and the super senior tranches' comportment.

Tranche		Original values in bps rel. to index tr.		G_{num} optimum place		gain	G_{time} optimum place		gain
a [1]	d [1]	$\mathbf{E}(X^{(\texttt{def})})$ [bps]	$\sigma(X^{(\texttt{def})})$ [bps]	ρ' $[\frac{\text{event}}{\text{year}}]$	$1/\lambda'$ $[\frac{1}{\text{event}}]$	value [1]	ρ' $[\frac{\text{event}}{\text{year}}]$	$1/\lambda'$ $[\frac{1}{\text{event}}]$	value [1]
0.00	0.03	58.6	115	0.20	0.11	3.0	0.08(5)	0.11	1.1
0.03	0.07	57.1	134	0.22	0.13	3.1	0.07(5)	0.13	1.1
0.07	0.10	30.8	88	0.23	0.16	3.5	0.07(0)	0.16	1.2
0.10	0.15	35.1	121	0.23	0.18	4.3	0.09(0)	0.17	1.5
0.15	0.30	39.1	202	0.25	0.27	9.3	0.11(0)	0.25	2.7
0.30	1.00	6.8	92	0.28	0.38	53.2	0.16(0)	0.34	12.4
0.00	1.00	227.7	606	0.23	0.18	6.0	0.11(0)	0.17	1.8

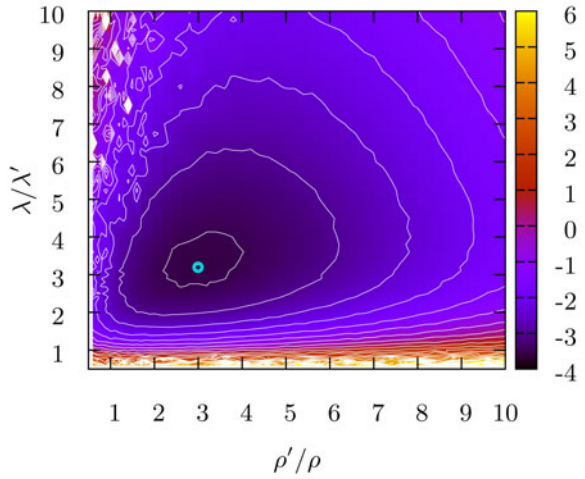

Fig. 9. (Color online) The magnitude of the gain $-\log_2 G_{\text{time}}$ for the super senior tranche in the `defPV` measurement, given in computational time as a function of the reweighting parameters: ρ' denotes the altered Poisson process intensity, $\frac{1}{\lambda'}$ the altered expected jump size. The real process uses the real world parameters described in (33) to (35). The variance decreases for the super senior tranche by increasing the intensity and the jump size to 2−4 times of their original value, but this is less significant than in Figure 8.

maps were intentionally left out. Already in the $\lambda/\lambda' \in [0.5, 1]$ region, a tendency of increasing variance can be observed. The $\rho'/\rho \in [0, 0.5]$ margins on the maps were left out, because decreasing ρ' below 0.5ρ results in even rarer events, thus higher variance, exceeding the current color scales.

In addition to the previous case, we have analyzed a more extreme, crisis-like situation where $\rho = 1\frac{\text{event}}{\text{year}}$. As anticipated, the gain in either number of paths or computational time is less spectacular, since even the original estimation was not as poor as with the previous, "calm" parameter set. This investigation showed that importance sampling has its limits: less than 75% saving was achieved for the super senior tranche even in the number of paths and at most 25% or nothing for the others, in contrast to the minimum of 66% that we have previously seen.

5 Conclusions

In this paper, we have shown the capabilities of importance sampling in estimating the fair price of CDO tranches. The simple model we covered, enabled us to check our results both analytically and by computer simulation. We showed that this approach is promising in pricing rare events, nevertheless, it has to be treated with care, since even in this basic model, singular behavior emerged. Furthermore, it has been shown that to speed up simulations, reducing the number of MC paths does not necessarily help if one thereby increases the computational time needed per path.

Future directions include testing the method for more elaborate models (such as [17] or [18]) and automatizing the optimization procedure, more specifically, gain a parameter set that simultaneously improves all standard tranches.

We would like to thank Morgan Stanley Hungary for the financial support. We are grateful to János Kertész and Bálint Tóth for the stimulating discussions. The work of B. V. was partially supported by OTKA (Hungarian National Research Fund) grant K 60708.

References

1. R.N. Mantegna, H.E. Stanley, *An Introduction to Econophysics: Correlations and Complexity in Finance* (Cambridge University Press, Cambridge, 2000)
2. R. Cont, Quant. Financ. **1**, 223 (2001)
3. R.N. Mantegna, J. Kertész, New J. Phys. **13**, 025011 (2011)
4. *Global CDO Market Issuance Data* (2010), `http://www.sifma.org/research`

5. M. Avellaneda, R. Buff, C. Friedman, N. Grandchamp, N. Gr, L. Kruk, J. Newman, Int. J. Theor. Appl. Finance **4**, 1 (2001)
6. R. Cont, A. Minca, Working Papers hal-00413730, HAL, 2008
7. J. Staum, State of the art tutorial II: simulations for financial engineering: efficient simulations for option pricing, in *Winter Simulation Conference* (2003), pp. 258–266
8. P. Glasserman, J. Li, New simulation methodology for risk analysis: importance sampling for a mixed Poisson model of portfolio credit risk, in *Winter Simulation Conference*, edited by S.E. Chick, P.J. Sanchez, D.M. Ferrin, D.J. Morrice (ACM, 2003), pp. 267–275
9. P. Glasserman, J. Li, Manage. Sci. **51**, 1643 (2005)
10. L. Capriotti, Quant. Financ. **8**, 485 (2008)
11. *Markit credit and loan indices*, Markit Group Limited
12. D.X. Li, Journal of Fixed Income **9**, 43 (2000)
13. F. Salmon, Recipe for Disaster: The Formula That Killed Wall Street (2009), http://www.wired.com/wired/issue/17-03
14. K. Giesecke, L.R. Goldberg, X. Ding, Oper. Res. **59**, 283 (2011)
15. X. Burtschell, J. Gregory, J.P. Laurent, Journal of Credit Risk **3**, 31 (2005)
16. X. Burtschell, J. Gregory, J.P. Laurent, Journal of Derivatives **16**, 9 (2009)
17. F.A. Longstaff, A. Rajan, J. Finance **63**, 529 (2008)
18. D. Brigo, A. Pallavicini, R. Torresetti, Risk magazine (2007), http://www.risk.net/risk-magazine/technical-paper/1500334/calibration-cdo-tranches-dynamical-gpl-model